Aerodynamic force coefficients of plain bridge cables in wet conditions

Matteoni, Giulia; Georgakis, Christos T.

Publication date:
2012

The Seventh International Colloquium on Bluff Body Aerodynamics and Applications (BBAA7)
Shanghai, China; September 2-6, 2012

Aerodynamic force coefficients of plain bridge cables in wet conditions

Giulia Matteoni[a,b], Christos T. Georgakis[b]

[a]*Department of Civil Enginering, Technical University of Denmark, Brovej, Building 118, Kgs. Lyngby, Denmark*
[b]*IPU, Building 404, Nils Koppels Allé, Kgs. Lyngby, Denmark*

ABSTRACT: In this paper, the aerodynamic forces and force coefficients from preliminary static wind tunnel tests on a plain cable in wet conditions are presented. The presented results are for several different relative cable wind-angles. A comparison is made with tests in dry conditions. In dry conditions, tests were performed for wind velocities between 2 and 31 m/s, whilst in wet conditions tests were performed for the range of wind velocities where rain rivulet formation was found possible, i.e. between 8-18 m/s. For all of the tested relative cable-wind angles in wet conditions, a reduction in the drag coefficient with increasing Reynolds number, accompanied by a near-zero lift coefficient, was observed. A theoretical evaluation of the aerodynamic damping assuming quasi-steady conditions reveals that changes in drag and lift coefficient are nonetheless not sufficient to generate negative aerodynamic damping. Analysis of the fluctuating lift component shows the presence of "enhanced" vortex shedding at specific wind velocities – similar to what might be observed in the presence of a tripping wire.

KEYWORDS: inclined bridge cable, yawed flow, drag, lift, rain, enhanced vortex shedding

1 INTRODUCTION

Rain-wind-induced vibrations (RWIVs) constitute 95% of all large amplitude vibrations of inclined bridge cables [1]. Vibrations may reach peak-to-peak amplitudes of 10 times the cable diameter, leading to serviceability issues and concerns over a much-decreased bending fatigue life for the cables. From both full scale and wind tunnel observations, it has been found that the vibrations occur mainly for cables declining in the wind direction, characterized by relative cable-wind angles Φ in the range of 60°-73°, under low to moderate rain intensities, in a restricted range of wind velocities of U = 5-18 m/s, and cable structural frequencies f = 0.6-3.3 Hz [2]. Physical parameters such as cable size and shape, surface roughness and wettability also affect the vibration mechanism [3]. Although the phenomenon is well known, the mechanisms that lead to this form of vibration are not thoroughly understood. Characterised by relatively low frequencies and large amplitudes of oscillation, RWIVs are generally not assumed to be a form of vortex-induced oscillation. Nevertheless, Matsumoto et al. [4] explained that wet bridge cables can undergo three types of unstable response, i.e. a "galloping type" which includes both divergent type galloping and velocity-restricted galloping, a "vortex shedding type" with a long period and a hybrid type. The galloping type response has been explained in terms of the negative slope in the lift coefficient with wind angle-of-attack, due to the formation of the upper water rivulet and/or the axial flow. Cosentino et al. [5] attributed RWIVs to the oscillation of the upper water rivulet on the vibrating cable model. They explained that during the cable's vibration cycle, the rivulet thickness, and the angular distance between the water rivulet and the stagnation line, changes as function of the cable's acceleration. When the rivulet reaches the farthest position from the flow stagnation line, it has gained its maximum thickness and the shear layer separating from the rivulet reattaches behind it, resulting in a single bubble on the cylinder surface. On the

other hand, when the upper rivulet is at the position nearest to the leading stagnation point, the rivulet thickness is minimum, and the shear layer separating from the rivulet does not reattach on the cylinder surface, leading to a flow pattern similar to that around a clean cylinder at a subcritical Reynolds number. Both explanations are inadequate though. For the stable formation of a balanced rain rivulet in the first case, cable wind angles-of-attack must remain in a very narrow range, thus eliminating the possibility for large changes in wind angle-of-attack. In the second case, the mechanism requires the relatively large oscillation of the cable, forfeiting any explanation of how the oscillation is initiated.

As RWIVs tend to occur for wind velocities that are generally lower than the maximum velocity used for the structural design of the cables and the bridge, the determination of the force coefficients of bridge cables in wet conditions has commonly been neglected. Nevertheless, these may vary significantly from those of dry cables. Furthermore, they may prove useful in the evaluation of the significance of the aforementioned additional effects in the mechanisms leading to RWIVs.

In the current work, the static forces and force coefficients of yawed full-scale bridge cable section models are determined from wind-tunnel tests, in both dry and wet surface conditions. From these tests, it is found that the measured forces on a wet cable differ from those of a dry cable. In particular, the drag coefficient is noticeably reduced, whilst the lift coefficient is near zero throughout the tested Re range – making the static cable model incapable of predicting negative aerodynamic damping. Furthermore, the fluctuating lift components are analysed and it is found that cable Strouhal numbers increase in wet conditions. Based on the measured drag and lift coefficients, as well as the observed Strouhal number, it is conjectured that the running water rivulets plays a similar role on the flow structure around the cable as a stationary tripping wire at a critical angular position from the flow stagnation line. Finally, the rain rivulet seems to generate a form of enhanced vortex shedding, which may contribute in some way to the initiation of the RWIV vibrations.

2 WIND TUNNEL TESTS

2.1 *Test setup*

Static wind tunnel tests were performed at the closed-circuit DTU/Force Climatic Wind Tunnel in Lyngby, Denmark. The wind tunnel features a test section of L×W×H =5m×2m×2m. Technical specifications of the wind tunnel are reported by Georgakis et al. [6]. The model (see Fig. 1) is a section of a prototype HDPE tube, with a nominal outer diameter of 160 mm, placed on an inner aluminium tube for increased stiffness. The measured roughness average of the cable model is R_a~1.8 μm. Aerodynamic forces at both cable ends were measured using 6-DOF force transducers, covered by HDPE dummy pieces of the same cable. For the tests performed in dry surface conditions, two configurations were tested, namely with and without end plates. When tested with end plates, the model was provided with circular end plates of diameter equal to 5 times the cable diameter, placed at a distance of approximately 90 mm from the walls, in order to minimize end effects. Wet tests were performed using the same model as in the dry state, but without end plates. At the upper end of the cable model, just above the measuring portion, two small diameter tubes were attached and connected to a water source placed outside the wind tunnel test chamber. In this way, a formed upper and lower water rivulet was simulated and allowed for a uniform rivulet along the full length of the cable model. Fig. 2 shows the test set-up in wet conditions. All tests were undertaken in smooth flow, i.e. for an along-wind turbulence intensity of I_u=0.5%, and for selected relative cable-wind angles Φ, defined as:

$$\Phi = \arctan\left(\frac{\sqrt{\tan^2\theta + \sin^2\beta}}{\cos\beta}\right) \qquad (1)$$

where θ is the vertical inclination and β is the horizontal yaw. In dry conditions, Φ=90º, 60º, and 55º were tested. In wet conditions, only Φ=60º and Φ=55º were investigated, as flow normal to the cable in wet conditions does not allow for the formation of a rain rivulet outside the wake. In dry conditions, the full wind tunnel velocity range up to 31 m/s was investigated. In wet conditions, the velocity range was restricted to the velocities at which rain rivulets could be formed, i.e. 8-18 m/s.

Figure 1. Full-scale, yawed cable model (dry tests).

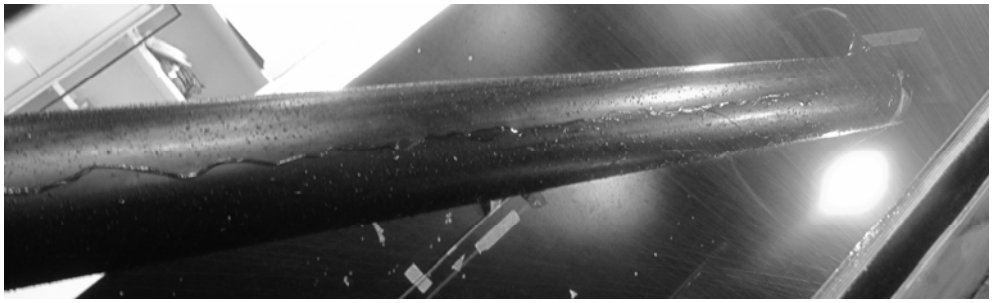

Figure 2. Full-scale yawed cable model (wet tests).

3 RESULTS

3.1 *Dry state*

The drag and lift coefficient components of dry inclined cables for the two selected relative cable-wind angles (Φ=60º and Φ=55º), together with cross-flow coefficients, are presented in Fig. 3. In cross flow, the blockage ratio was 8%, thus leading to the need for a drag coefficient correction following the Maskell III Method [7]. For the yawed cable tests, the wind tunnel blockage was lower than 2% and therefore no correction was needed.

The cable's aerodynamic damping is determined according to the general expression derived by Macdonald and Larose [8] for small (1-DOF) vibrations of a cylinder in a given plane. For

across-flow vibration (α=90°) and along-flow vibration (α=0°) the aerodynamic damping reduces to equations (2) and (3) respectively:

$$\xi_a = \frac{\mu \mathrm{Re}}{4m\omega_n} \frac{1}{\sin\phi}(C_D + \frac{\partial C_L}{\partial \alpha}) \qquad (2)$$

$$\xi_a = \frac{\mu \mathrm{Re}}{4m\omega_n}(2C_D \sin\phi + \frac{\partial C_D}{\partial \mathrm{Re}} \mathrm{Re} \sin\phi + \frac{\partial C_D}{\partial \phi}\cos\phi) \qquad (3)$$

where C_D, C_L are the cable's drag and lift coefficients, respectively, α is the wind angle-of-attack, Φ is the relative cable-wind angle, μ is the dynamic viscosity, m is the cable's mass and ω_n is the cable's circular frequency.

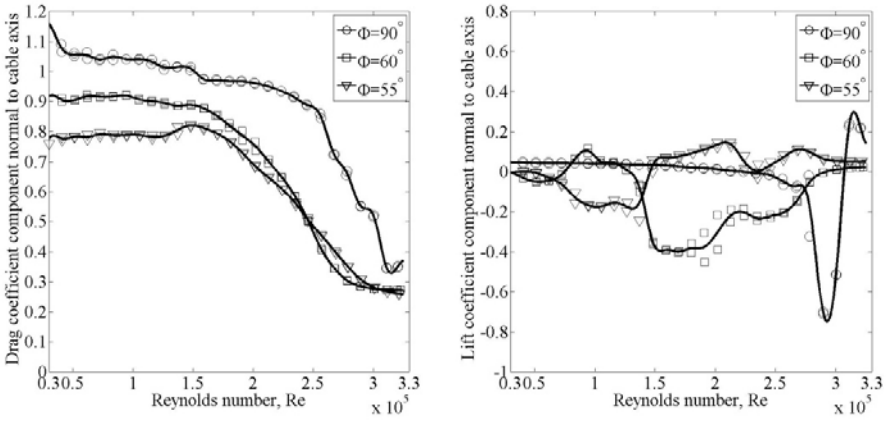

Figure 3. Drag and lift coefficient components for full-scale yawed cable model in dry conditions with end plates.

The across-flow (left) and along-flow (right) aerodynamic damping, normalized by the factor ($\mu/(4m\omega_n)$) and based on the drag and lift coefficient components in Fig. 3, are shown in Fig. 4. By neglecting the variation of the lift coefficient with angle-of-attack, the predicted across-flow aerodynamic damping is positive through the tested range of Reynolds number for all tested geometries. Similarly, neglecting the variation of the drag coefficient component with relative cable wind angle, leads to negative aerodynamic damping for Re=2.55×10^5-3.18×10^5 (Φ=90º), Re=2.27×10^5-2.83×10^5 (Φ=60º), Re=2.35×10^5-3.01×10^5 (Φ=55º).

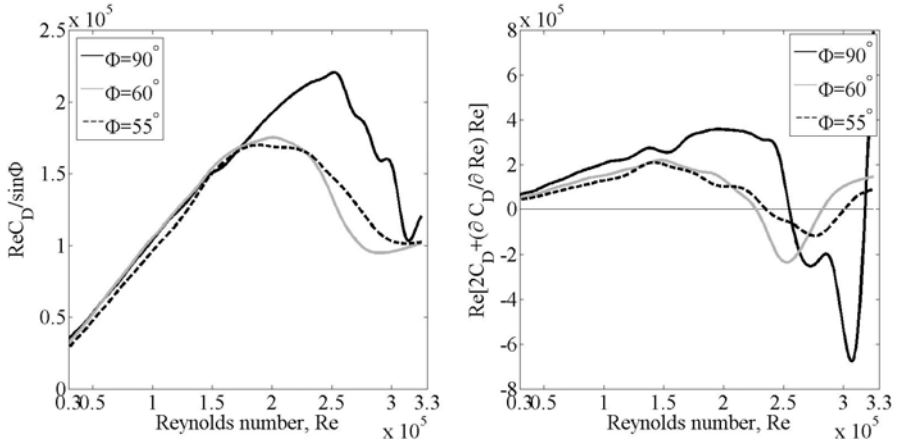

Figure 4. Across-flow and along-flow normalized aerodynamic damping for yawed cable model (dry conditions).

In Fig. 5, the drag and lift coefficient components for yawed cable models in dry conditions and in the absence of end plates are presented, for relative cable wind angles of Φ=90°, 60º and 55°. For all tested relative cable-wind angles, Φ, the drag and lift coefficient components are significantly changed in the absence of end plates. It is believed that varied three dimensional flow conditions must thus be responsible for the change in the aerodynamic behavior of the cable models, particularly when yawed. From Fig. 5 it is in fact observed that for flow normal to the cable axis, i.e. Φ=90º, the drag coefficient decreases through the full tested range of Reynolds numbers. For the yawed cases, the drag coefficient component normal to cable is continuously decreasing for Reynolds numbers higher than Re=1.61×10^5 (Φ=60º) and Re=1.06×10^5 (Φ=55º).

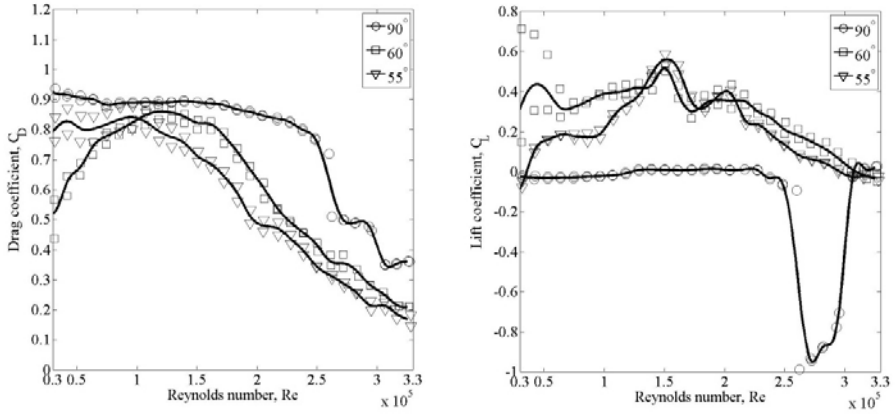

Figure 5. Drag and lift coefficient components for yawed cable model (dry conditions, no end plates).

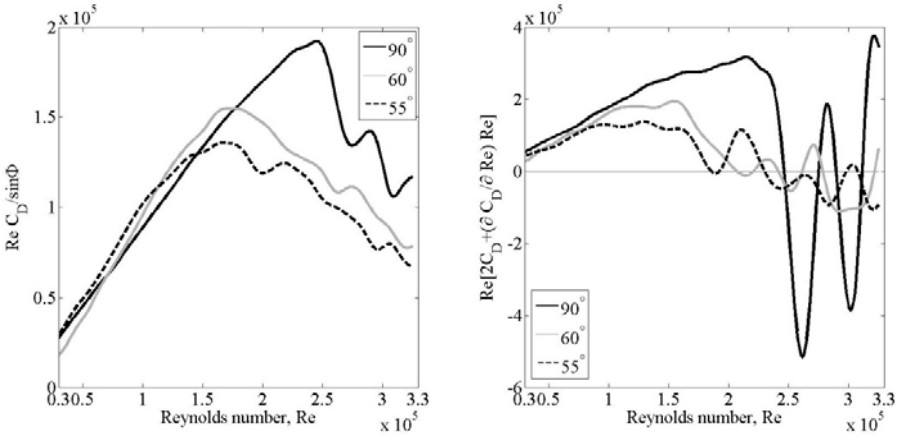

Figure 6. Across-flow and along-flow normalized aerodynamic damping for yawed cable model (dry conditions, no end plates).

Fig.6 is similar to Fig. 4, except that the results are for the dry tests with no end plates. Due to discontinuities in the slope of the drag coefficient components in the critical Re range, a change in the sign of the normalized aerodynamic damping is experienced. Negative aerodynamic damping is predicted for Re=2.46×10^5-2.75×10^5 and Re=2.90×10^5-3.11×10^5 (Φ=90º), Re=2.06×10^5-2.21×10^5 and Re=2.41×10^5-2.61×10^5 (Φ=60º), Re=1.86×10^5-1.92×10^5 and Re=2.30×10^5-2.98×10^5 (Φ=60º).

3.2 *Wet state*

In wet conditions, upper and lower water rivulets form when the wind velocity reaches the value of U=8 m/s (Re=0.80×10^5). This can be understood as the velocity at which there is a balance between the gravitational and the aerodynamic forces acting on the rivulet. At this stage the rivulets follow a slightly sinusoidal trajectory along the cable length. As the wind velocity is increased, the rivulets trajectory changes to a straight line. When the wind velocity overcomes the value of U=18 m/s (Re=1.8×10^5) the rivulets are disrupted, as all water is blown off of the cable.

Due to the presence of the water rivulets, the total force measured on the cable section at any time is comprised of an aerodynamic component and a gravitational component, as a result of the added weight of the water on the cable surface. The latter contribution was estimated based on the visually observed width and thickness of the upper and lower water rivulets along the cable length, which were equal to approximately 20 mm by 2 mm. This is in agreement with previous accounts, where the water rivulet base carpet width and hump height were estimated, depending on the rain intensity, to be in the range of 8-38 mm and 0.5-2mm, respectively, [9]. Thus, by assuming as observed that the weight of the water rivulets remains constant throughout the range of wind velocities - from their formation up to their disruption - the total added weight of water is 1 N/m. The drag and lift force components normal to the cable for relative cable-wind angle Φ=60° are presented in Fig. 7.

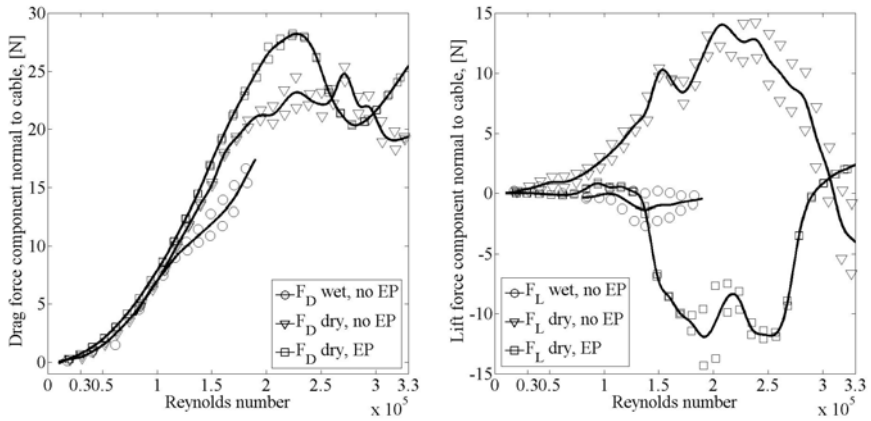

Figure 7. Drag (left) and lift (right) force component normal to cable (Φ=60º). EP refers to 'end plates'

For the dry tests with varying end conditions, it can be observed that the drag force components normal to cable generally follow each other in the subcritical Re range. Major deviations are observed though for Reynolds numbers higher than Re~1.6×10^5, i.e. in the critical Reynolds number range. In wet conditions, the drag force component normal to cable is generally equal to or lower than the respective force component in dry conditions, whilst the lift force component is near zero.

The drag and lift forces normal to the cable for relative cable-wind angle Φ=55° are reported in Fig. 8. Note that in wet conditions, for both Φ=60° and 55°, the total and purely aerodynamic force components do not differ significantly from each other, as the contribution of the projection of the added gravitation water weight along the two force components is lower than 0.52 N/m. Moreover, for Φ=55°, the angle between the gravitational force and the lift force component is 90°, thus making the total and the lift force components equal. The aerodynamic force components in wet conditions have been converted into aerodynamic force coefficients and presented in Figs. 9-10. In these figures, the drag and lift coefficient components normal to the cable axis obtained in wet surface conditions (with end plates) are compared with the respective force

components in dry surface conditions (with and without end plates) for the two yawed cable models.

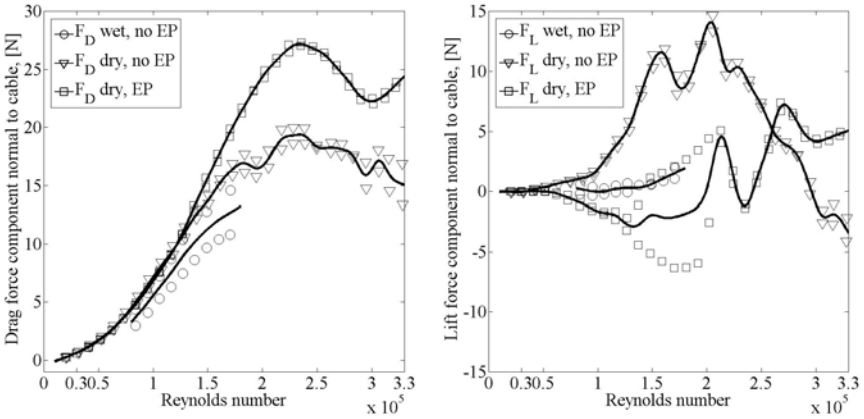

Figure 8. Drag (left) and lift (right) force component normal to cable (Φ=55º). EP refers to 'end plates'.

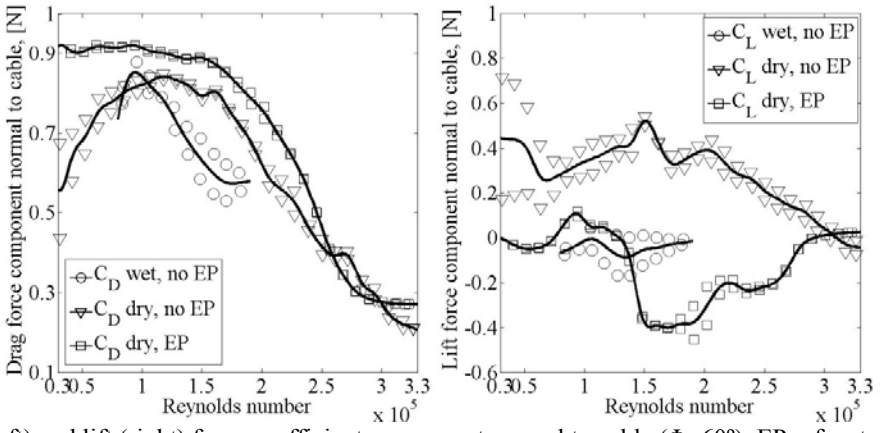

Figure 9. Drag (left) and lift (right) force coefficient component normal to cable (Φ=60º). EP refers to 'end plates'.

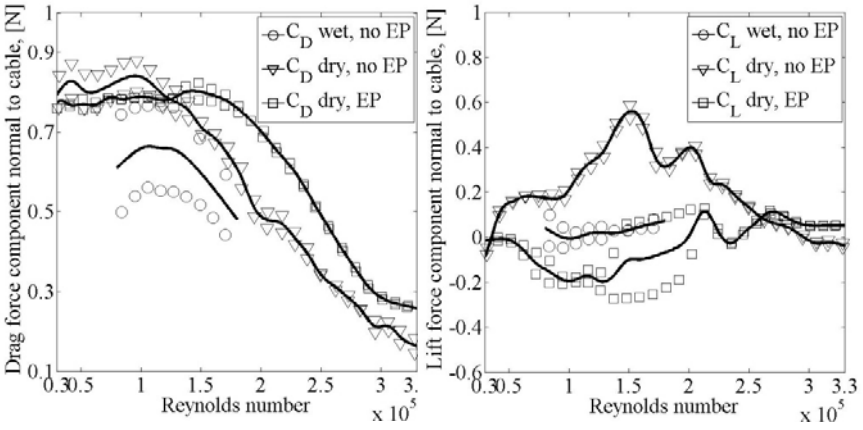

Figure 10. Drag (left) and lift (right) force coefficient component normal to cable (Φ=55º). EP refers to 'end plates'

In Figs. 11 and 12, the along-wind and across-wind normalized aerodynamic damping obtained in wet conditions (with end plates) and dry conditions (with and without end plates) for the two yawed cable models, is shown. For the case of Φ=60°, the across-wind and along-wind aerodynamic damping follows the same tendency as for the dry state, but it exhibits lower values. For

the case of Φ=55°, even if positive, the aerodynamic damping in wet conditions doesn't follow the same tendency as for the other tested cases in dry conditions.

It is apparent that the presence of water rivulets on a static yawed cable leads to a change in the flow structure around the cable (and thus in the drag and lift coefficient components), but it is not sufficient in itself to predict negative aerodynamic damping.

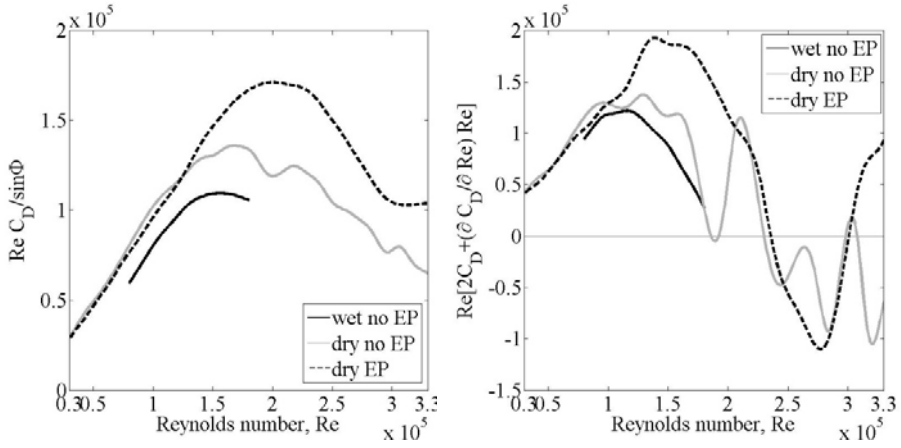

Figure 11. Across-wind (left) and along-wind (right) normalized aerodynamic damping for yawed cable model (Φ=60°). EP refers to 'end plates'

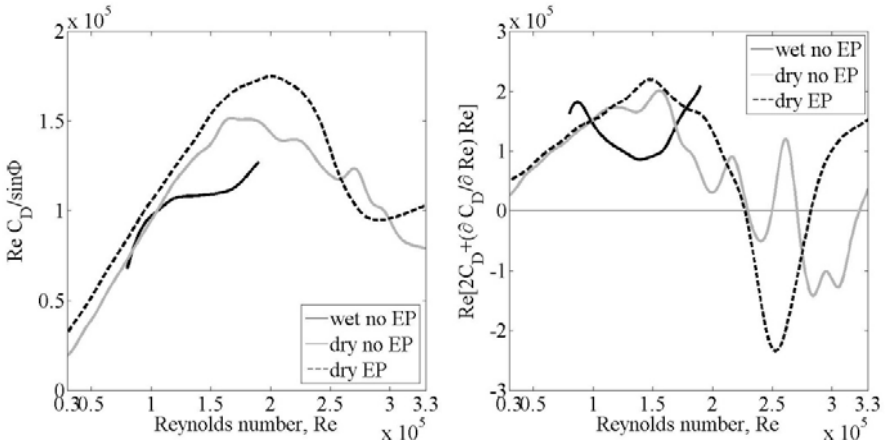

Figure 12. Across-wind (left) and along-wind (right) normalized aerodynamic damping for yawed cable model (Φ=55°). EP refers to 'end plates'

3.3 *Vortex shedding*

The RMS (Root Mean Square) values of the lift component normal to the cable (i.e. fluctuating lift) for varying Re values are reported in Fig. 13. For Φ=60° it is observed that in dry conditions the fluctuating lift coefficient exhibits an increase for Re~1.0-3.0×10^5, in both the presence and absence of end plates. In wet conditions, the fluctuating lift component peaks at between Re=1.3-1.4×10^5, whilst for Φ=60°, the fluctuating lift is considerably higher than in dry conditions, represented a form of enhanced vortex shedding. The same phenomenon, i.e. increase of the fluctuating lift for wet cylinders in comparison to the dry state, has been previously reported for the range of Reynolds numbers where the upper water rivulet reaches a critical angular position from

the flow stagnation line, but albeit for much lower Re numbers that examined here [10]. The increased RMS of the fluctuating lift for Φ=60° also qualitatively resembles the increased RMS response observed in certain cases when a cylinder is fitted with a flow tripping wire [11]. As it is unclear what initiates the RWIV, it is conjectured that the observed enhanced vortex shedding may trigger a response in higher cable harmonics or sub-harmonics. The driving mechanism may then migrate from vortex shedding to an aeroelastic mechanism.

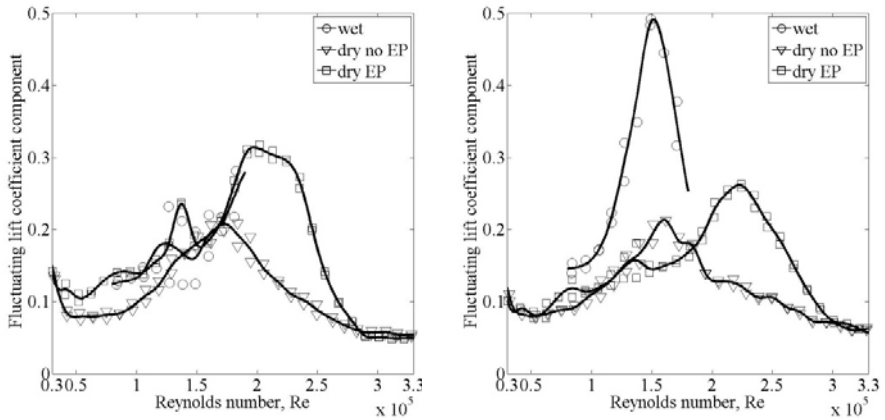

Figure 13. RMS fluctuating lift coefficient component normal to cable for Φ=60° (left) and Φ=55° (right).

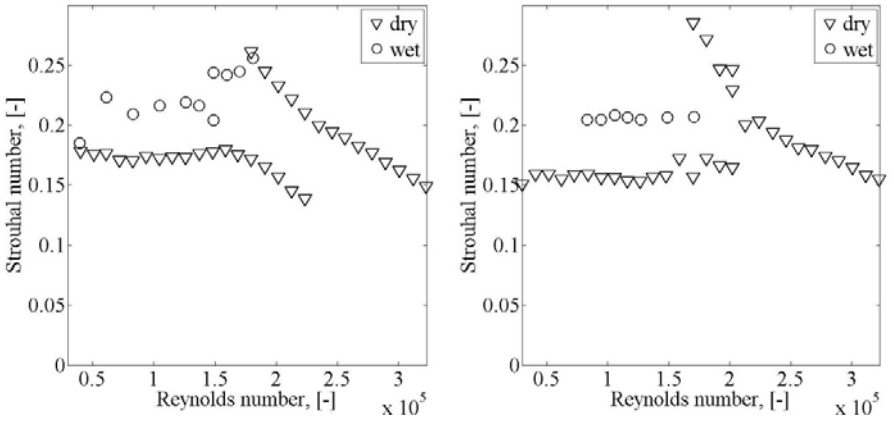

Figure 14. Strouhal number versus Reynolds number, Φ=60° (left) and Φ=55° (right), dry and wet conditions.

The Strouhal number versus Reynolds number is plotted for all of the tests in Figure 14. A linear trend is observed between the Strouhal frequency and Reynolds number in the PSD (power spectral density) of the lift coefficient component normal to cable for Φ=60° and Φ=55° in dry conditions, which disappears for Re~1.6x10^5 for both Φ=60° and Φ=55°. Additionally, in dry conditions and in the critical Reynolds number range, the lift's PSD exhibits local peaks at two separate Strouhal frequencies. In wet conditions, the same linearity is evident only for the test case Φ=55° throughout the full tested Re range. Moreover, in dry conditions, for both Φ=60° and Φ=55°, and for Reynolds numbers marking the start of the critical range (i.e. Re~1.6x10^5), local peaks in the PSD are observed for frequencies near zero. These may be associated with the occurrence of an alternating single separation bubble on one side of the cylinder, as reported by Nikitas et al. [12]. Finally, for both Φ=60° and Φ=55°, the Strouhal numbers measured in wet conditions are higher than in dry conditions and between 0.2 and 0.25. Again, this might be ex-

pected of a stationary cylinder with tripping wire fitted at a critical angular position from the stagnation line [11], [13].

4 CONCLUSION

Static forces and force coefficients of yawed full-scale bridge cable section models are determined from wind-tunnel tests, in both dry and wet surface conditions. In dry conditions, tests are performed for wind velocities between 2 and 31 m/s, while in wet conditions they are performed for wind velocities between 8 and 18 m/s. For the tested relative cable-wind angles, it is found that the drag coefficient of cables in wet conditions is reduced compared to a dry cable and the lift coefficient is near zero throughout the tested Re range. The changes in the aerodynamic coefficients in the range of Reynolds numbers in which the water rivulet can form cannot predict the generation of negative aerodynamic damping. Moreover, in wet conditions, the cable's Strouhal numbers are increased when compared to a dry cable. Based on the trend on the drag and lift coefficient, as well as of the Strouhal number, it is suggested that the running water rivulets plays a similar role on the flow structure around the cable as a stationary tripping wire fitted on the cable's surface. Finally, it is conjectured that an observed enhanced vortex shedding may contribute to the initiation of RWIV.

5 ACKNOWLEDGEMENTS

The authors would like to thank Femern A/S and Storebælt A/S for their financial support without which this work would not have been possible.

6 REFERENCES

1 P. Wagner, J.P. Fuzier, Health monitoring of structures-which solutions. Dissemination of the results of the IMAC European Project. 5th Int. Symposium on Cable Dynamics, Santa Margherita Ligure, 2003, pp. 333-340.
2 N.J. Gimsing, C.T. Georgakis, *Cable Supported Bridges, Concept and Design*, 3rd Edition, Wiley, 2012
3 O. Flamand, Rain-wind induced vibration of cables. J. Wind Eng. Ind. Aerodyn., 57 (1995) 353-362.
4 M. Matsumoto, T. Saitoh, M. Kitazawa, H. Shirato, T. Nishizaki, Response characteristics of rain-wind induced vibration of stay-cables of cable-stayed bridges. J. Wind Eng. Ind. Aerodyn. 57 (1995) 323-333.
5 N. Cosentino, O. Flamand, C. Ceccoli, Rain-wind induced vibration of inclined stay cables. Part I: Experimental investigation and physical interpretation. J. Wind and Structures, 6, (2003), 471-484.
6 C.T. Georgakis, H.H. Koss and F. Ricciardelli, Design specifications for a novel climatic wind tunnel for testing of structural cables, Proc. 8th Int. Symposium on Cable Dynamics, Paris, 2009, pp. 333-340.
7 K. Cooper, E. Mercker, J. Wiedemann, Improved blockage corrections for bluff bodies in closed and open wind tunnels., 10th International Conference Wind Engineering, Copenhagen, 1627-1634.
8 J.H.G. Macdonald, G.L. Larose, A unified approach to aerodynamic damping and drag/lift instabilities, and its application to dry inclined galloping. J. Wind Eng. Ind. Aerodyn., 22 (2006) 229-252.
9 C. Lemaitre, E. de Langre, P. Hémon, Rainwater rivulets running on a stay cable subjected to wind. European J. of Mechanics B/Fluids, 29 (2010) 251-258.
10 MD. Mahbub Alam, Y. Zhou, Turbulent wake of an inclined cylinder with water running. J. Fluid Mech. 58 (2007) 261-303.
11 F.S. Hover, H. Tved, M.S. Triantafyllou, Vortex-induced vibration of a cylinder with tripping wires. J. Fluid Mech. 448 (2001) 175-195.
12 N. Nikitas, J.H.G. Macdonald, J.B. Jakobsen, T.L. Andersen, Critical Reynolds number and galloping instabilities: experiments on circular cylinders, Experiments in Fluids, 52 (2012) 1295-1306
13 T. Igarashi, Effect of Tripping Wires on the Flow around a Circular Cylinder normal to an Airstream. Bulletin of JSME, 29 (1986) 2917-2924.